Journal of Materials and Environmental Sciences
ISSN : 2028-2508
CODEN : JMESCN

J. Mater. Environ. Sci., 2018, Volume 9, Issue 3, Page 902-908

https://doi.org/10.26872/jmes.2018.9.3.100

http://www.jmaterenvironsci.com

Green Synthesized Optically Active Organically Capped Silver Nanoparticles using Stem Extract of African Cucumber (*Momordica charantia*)

Anuoluwa Abimbola Akinsiku[1], Enock Olugbenga Dare[2], Kolawole Oluseyi Ajanaku[1*], Joseph Adeyemi Adekoya[1], Joan Ayo-Ajayi[1]

1. Chemistry Department, College of Science & Technology, Covenant University, Km. 10, Idiroko Road, Canaan Land, Ota, Ogun State, Nigeria

2. Department of Chemistry, Federal University of Agriculture Abeokuta, PMB 2240, Alabata Road, Abeokuta, Nigeria.

Received 25Oct 2016,
Revised 22Feb 2017,
Accepted 27Feb 2017

Keywords

- ✓ Silver nanoparticles;
- ✓ African cucumber;
- ✓ optical property;
- ✓ absorption;
- ✓ emission

K.O. Ajanaku
kola.ajanaku@covenantuniversity.edu.ng

Tel. :+2348033575624

Abstract

Silver nanoparticles (Ag NPs) were synthesized by a rapid facile plant-mediated green route. Sustainable and renewable stem extract of locally sourced African cucumber acted as reducing/capping agent, an alternative to toxic chemicals. The phytochemical screening indicated the existence of saponins and alkaloids in the stem extract of *M. charantia.* Unprecedented nucleation and growth of Ag NPs commenced within 5 minutes of the reaction. The mechanism of reaction was considered to be diffusion controlled Ostwald ripening process. Optical property of the as prepared Ag NPs was characterized by high intensity of absorption, revealed by narrow intense peaks, stipulating confinement of excitons. Surface Plasmon Band (SPB) of Ag NPs appeared at 400 - 460 nm. Photoluminescence (PL) excitation of the Ag NPs at 329 nm exhibited excitonic emission at 440 nm. The Ag NPs portrayed quasi-spherical shapes, with a mean size of 27.81 ± 1.64 nm from Transmission Electron Micrograph (TEM) measurement. XRD measurement showed peaks indexed to fcc Ag with a particle diameter of 25 nm, which corroborated TEM measurement. Elemental mapping of the nanoparticles showed an orientation of the Ag NPs, an evidence of capping by the biomolecules which stabilized the newly formed Ag NPs. Fourier Transformed Infra-red (FTIR) analysis showed the presence of hydroxyl groups (−OH) stretching, (−CH) stretching, C=C stretching and C−N group (in the phytochemicals) at 3237, 2913, 1620 and 1021 cm^{-1} respectively. It can be inferred that the as prepared Ag NPs is an optically active material.

1. Introduction

Unique properties of nanostructured materials qualify them for various applications, such as sensor, electronics, optical devices and many more. Silver nanoparticles are widely synthesized and investigated for optical and antimicrobial properties using various methods. Optical property of nanomaterials with diverse anisotropic shapes is applied in optoelectronics and photonic devices. This optical property, amongst others is usually exhibited by materials whose metal film thicknesses decrease as new materials with different appearance from the bulk emerge. This tuning of property by manipulating the nanostructure of materials is of great applications in the field of nanochemistry today. Excitation of surface plasmons which are strongly bound to the incident surface is one of the observable changes when metal surface is exposed to electrons or photons. Surface Plasmon Resonance (SPR) detection method is applicable as one of the methods of studying biological interactions in nature [1]. Moreover, the optical property of any nanostructure depends on its shape and composition, which leads to the synthesis and fabrication of different nanostructure of diverse shapes and functionalities [2-4]. Metal nanoparticles with sizes above 5 nm radius (critical value) are considered to display red shift of SPR, which increases as particle size increases. Thus, varying particles sizes can tune the SPR, as this ability is useful for optimizing surface-enhanced effects and biosensing response of nanostructures. This red shift of SPR peak influenced by refractive index of metal nanostructures and noble metal nanoparticles of various shapes form the basis of sensing application. Quite a number of literature reveal high sensitivity of larger nanostructures with peak broadening effect due to multipolar excitations, but the sharp peaks of these nanoparticles produce a red shift in their plasmon resonance. Further work done has also shown thatconcentration, size and distribution of nanoparticles could be measured using optical absorption of colloidal

solutions [5]. It is obvious that metallic nanomaterials are being focused as optically active materials based on their absorption, nonlinear properties and photoluminescence emission. Thus, quantum confinement effect by nanomaterials having small particle sizes significantly enhances their optical emission [6-7].
Several literatures have reported silver nanoparticles with optical properties synthesized using chemical methods. Meanwhile, fewer investigations have been carried out on green plant-mediated synthesis of Ag nanoparticles. Some recognized contributions involve the use of fungi [8], extracellular yeast [9-11], marine algae or eukaryotic autotrophs [12] and green plants [13]. In all the findings, plant-mediated green synthesis is considered facile, cost effective and environmentally friendly compared to conventional synthesis of metallic nanoparticles which involves complex procedures.
In this work, Ag NPs was synthesized by reduction of Ag^+ with stem extract of locally sourced African cucumber instead of commonly used leaf extract. The absorption and emission properties of the as synthesized silver nanoparticles were studied. The phytochemicals present in the plant extract were considered as reducing and capping agents for the newly formed nanoparticles. The biosynthesized Ag NPs were characterized using UV-Visible and PL spectrophotometry, scanning electron microscopy (SEM), transmission electron microscopy (TEM), Fourier transform infrared (FTIR), X-ray diffraction (XRD) and selected area electron diffraction (SAED).

2. Experimental details

2.1. *Materials*

Momordica charantia stem extract (African Cucumber), $AgNO_3$ commercially obtained from Sigma-Aldrich, distilled deionized water.

2.2. *Preparation of leaf extract*

African cucumber plant was collected during early hours before sunrise from a garden at Atan-Iju, Ogun State, Nigeria. The plant was identified and authenticated at Forest Research Institute of Nigeria (FRIN) with voucher specimen, FHI 109926 deposited at the herbarium headquarters, Ibadan, Nigeria. Stem of the plant was chopped, homogenized using mortar and pestle and then extracted with water (1:5 wt/v). The organic extract was filtered with Whatman no. 1 filter paper, after which, the filtrate was collected and preserved at 4 ^oC for phytochemical screening and Ag nanoparticles synthesis. The phytochemical screening of the plant extracts was carried out according to literature [14].

2.3 *Synthesis of Silver Nanoparticles using Stem Extract of Momordica charantia*

Filtrate of the stem extract (10 mL) was added to 100 mL of $AgNO_3$ solution (precursor) at varying concentrations (0.5 - 3.0 mM). The resulting mixture was heated up to 70^oC for 30 minutes. A double beam thermo scientific GENESYS 10S model UV-Vis spectrophotometer (1 cm path length quartz cuvette operated at a resolution of 1 nm) was used to monitor bioreduction of Ag^+ to Ag^0, as aliquot samples were collected at different time intervals [15]. Colour change and absorption maxima which signaled reduction of Ag^+ were fully monitored.

2.4 *Isolation of the Ag NPs*

Nanoparticles were separated from the reaction mixture by centrifugation and numerous washing using distilled deionized water. The biosynthesized nanoparticles were collected using centrifuge model 0508-1; operated at 5000 rpm for 30 minutes. For purification, nanoparticles suspension was re-dispersed in distilled deionized water so as to remove unbounded organics. It was finally centrifuged at 5,000 rpm for 10 minutes; vacuum dried and kept for further characterizations.

2.5 *Characterization*

2.5.1 *Optical Characterization*

Double beam thermo scientific GENESYS 10S model UV-Vis spectrophotometer was used to carry out the optical measurements. Samples were taken at different time intervals and placed in quartz cuvette of 1 cm path length, operated at a resolution of 1 nm, using distilled deionized water as a reference solvent. A Perkin-Elmer 55 spectrometer was used to measure the photoluminescence of the green synthesized Ag nanoparticles. The samples were placed in quartz cell (1 cm path length).

2.5.2. *Structural Characterization*

Crystallinity of the Ag NPs was analyzed using X-ray diffraction (XRD), BrukerAXS D8 diffractometer equipped with nickel filtered Cu Karadiation (k=1.5418 Å) at 40 kV, 40 mA, 25^oC, scanning rate of 0.05^o min^{-1} in 2 hoursrange from20^0 to 80^0. The detailed structural and morphological characteristics, particle size

determination were verified with Technai G2 transmission electron microscope (TEM) coupled with an energy-dispersive X-ray spectrometer (EDX), operated at an accelerating voltage of 200 KeV and 20 µA current. Samples for TEM analysis wereprepared by drop-coating Ag NPs suspensions onto carbon-coated copper TEM grids. Films on the TEM grids were allowed to stand for 2 minutes, after which the extra solution was removed using a blotting paper and the grid allowed drying prior to measurement. Possible functional groups which may support existence of capping and stabilization were identified by Perkin-Elmer 100 series FT-IR which functioned at 4 ms^{-1} scan rate over the range of 4000-500 cm^{-1} wave number, in the diffuse reflectance mode at a resolution of 4 cm^{-1} in KBr pellets.

3. Results and Discussion

3.1. *Optical Properties of Ag NPs*

Synthesis of monometallic Ag NPs by facile reduction with stem extract of African cucumber was done at varying precursor solution concentrations. The onset of nucleation and growth began within 5 minutes of reaction, as there was significant absorption by the prepared nanoparticles at different concentrations in the wavelength range 400 - 440 nm which is distinctive of silver NPs [16]. The observed blue shift wavelength appearing at 412 nm was a result of strong quantum confinement effect, with corresponding absorption intensity of 1.311a.u. which increased with reaction time without further shift in maximum wavelength.

The observed colour changed from light brown to deep brown. Figure 1a represents $AgNO_3$ solution (i), initial colour of $AgNO_3$ with the extract (ii) and final colour change after reduction (iii).

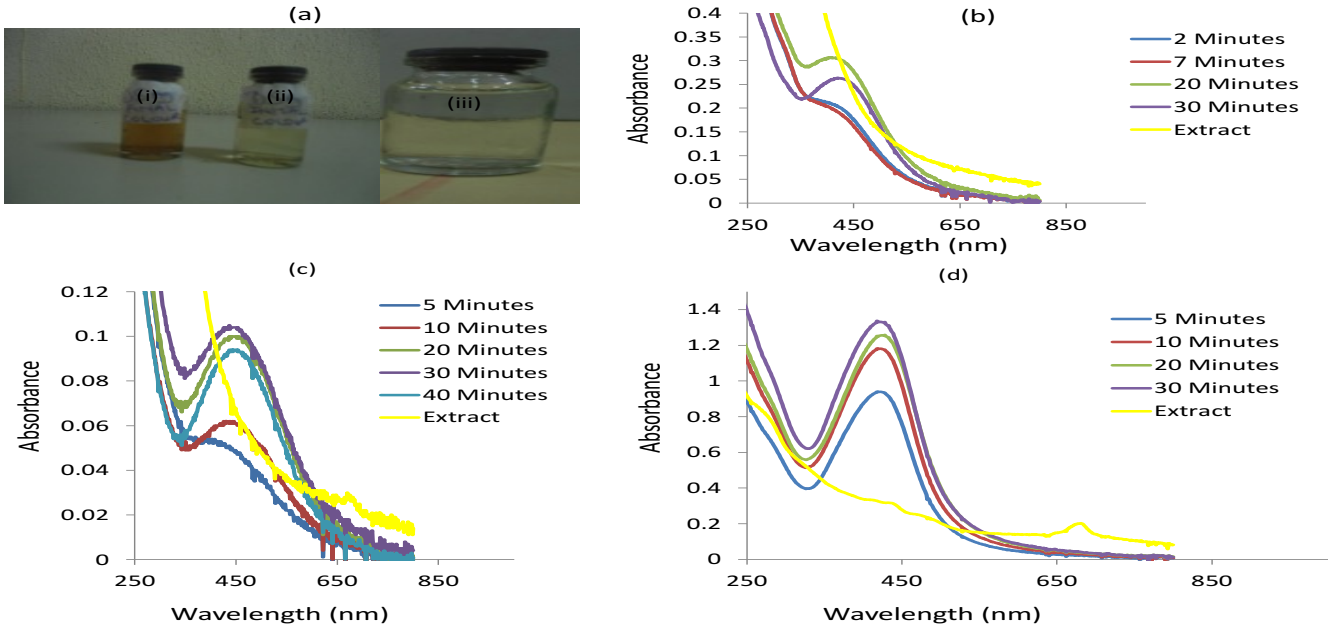

Figure 1:(a) The final silver dispersion formed after reduction (i), $AgNO_3$ solution with *Momordicacharantia* stem extract before reduction (ii), and $AgNO_3$ solution (iii). UV-Vis spectra of Ag NPs prepared from (b) 1.0 mM (c) 2.0 mM (d) 3.0 mM $AgNO_3$ solution at 70°C.

The red shift detected in the surface plasmon band was an indication of size increment due to capping of the newly formed nanoparticles by the biomolecules. Significant bio-reduction occurred with extract of *M. charantia* stem signifying that adequate phytochemicals (saponins and alkaloids) were present in stem part of the biomass used [17].

Photoluminescence (PL) spectrum of Ag NPs obtained by the reaction of *M. charantia* stem extract and $AgNO_3$ precursor solution at 70°C is presented in Figure 2. The spectrum was characterized by a single, strong intensity peak, making it a potential material for optical application [18].

For an excitation at 322 nm there was an emission at 443 nm. Stoke's shift was observed as a result of energy loss between the excitation and emission of fluorophores [19]. The symmetry between absorbance and fluorophores spectra (Figure 3) of the Ag NPs showed mirror image relationship [20].

3.2 *Morphology of Ag nanoparticles*

The selected area electron diffraction (SAED) pattern, particle size distribution histogram and TEM micrograph of the Ag NPs formed by the stem extract of*M. charantia* are presented in Figure 4 (a), (b) and (c) respectively.

Other representative TEM images of Ag NPs derived from *M. charantia* stem extract are shown in Fig. 5. The particles size ranged from 15 - 40 nm, with a mean diameter of 27.81 ± 1.64 nm. The size distribution histogram (Fig. 4b) shows relatively uniform particle sizes, which is an advantage of plant-mediated green synthesis. TEM image of the nanoparticles portrayed aggregates of quasi-spherical and nanocubes with irregular contour due to self-assembly.

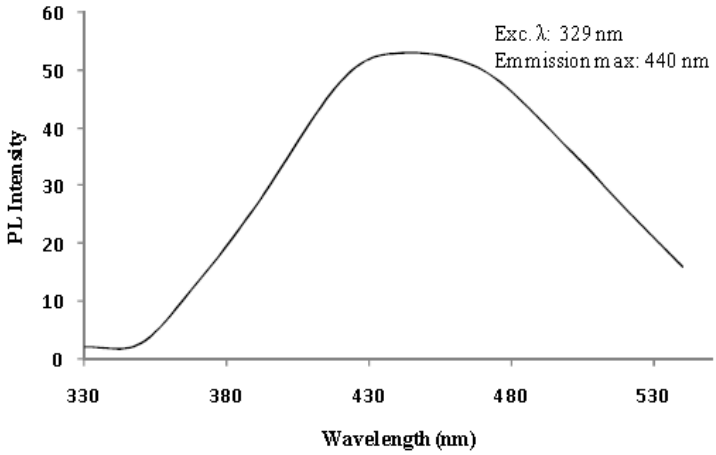

Figure 2: PL emission spectrum of Ag NPs synthesized using *M. charantia*stem extract

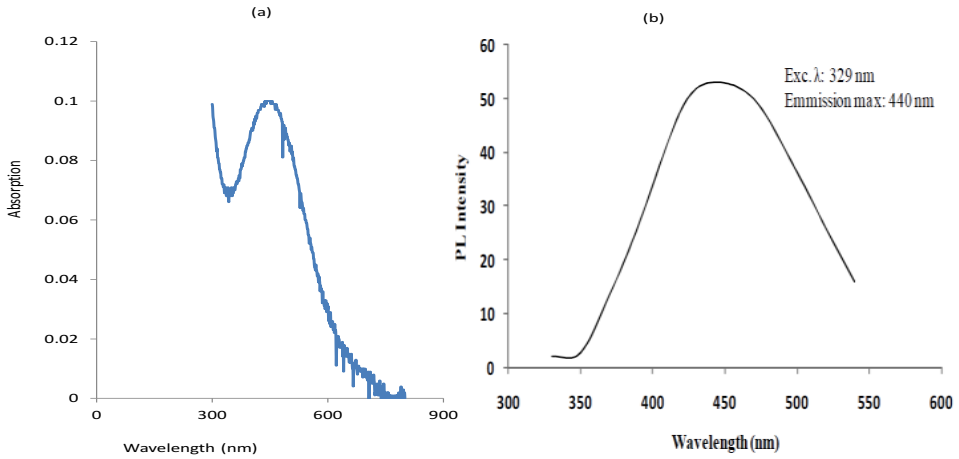

Figure 3: Uv-Vis absorbance (a) and PL emission (b) spectrum of biosynthesized Ag NPs

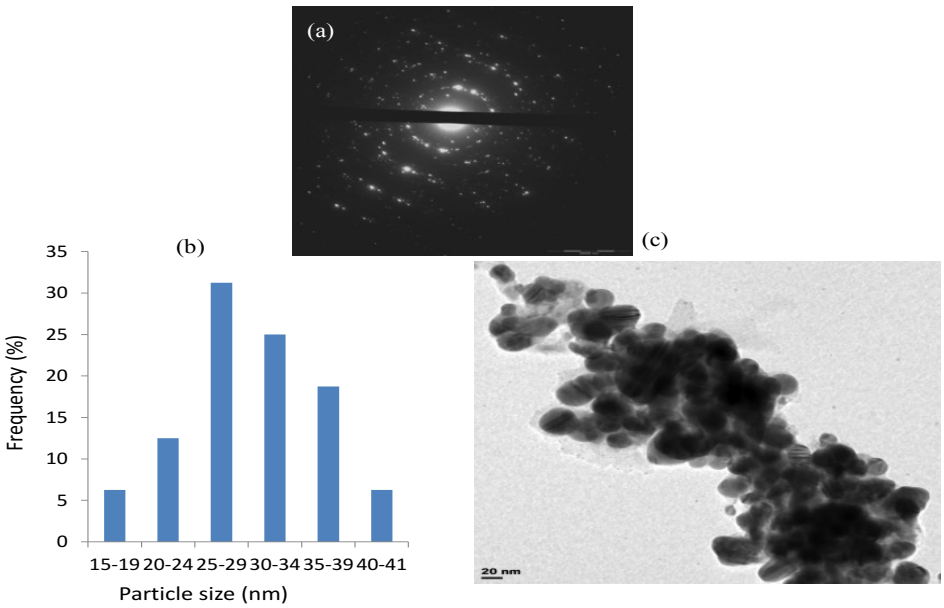

Figure 4: (a) SAED pattern of the Ag NPs (b) Particle size distribution histogram of Ag NPs determined from TEM image (c) Representative TEM image of the Ag NPs

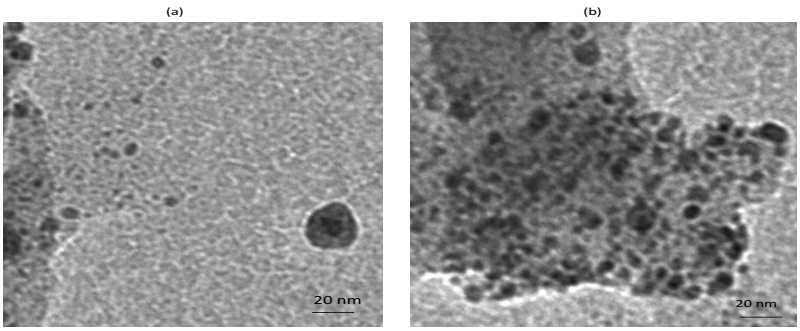

Figure 5: (a, b): Representative TEM images of Ag NPs derived from *M. charantia* stem extract

Figure 6 is an elemental mapping of the Ag NPs obtained from TEM micrograph showing orientation of Ag nanoparticles. It is an evidence to support capping of the newly formed nanoparticles by biomolecules, as demonstrated by the diagonal orientation. The SAED ring pattern was indexed to (111), (200), (220) and (311) of Ag metals with fcc structure. Hence, this verified the crystalline phases of the Ag NPs. The result of the EDX analysis signified the presence of significant amount of Ag with the atomic composition of 71.37% in the nanoparticle (Figure 7).

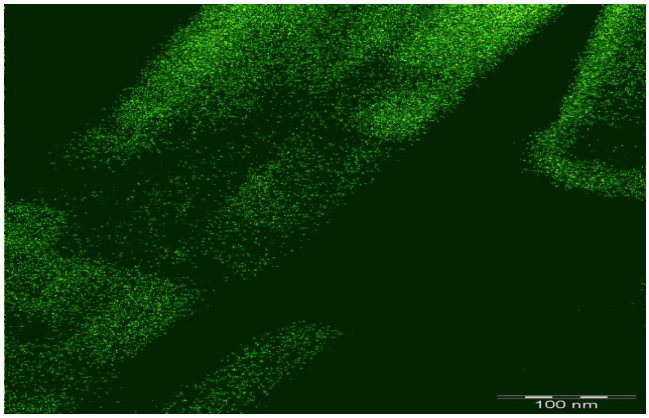

Figure 6: Elemental mapping of the Ag NPs

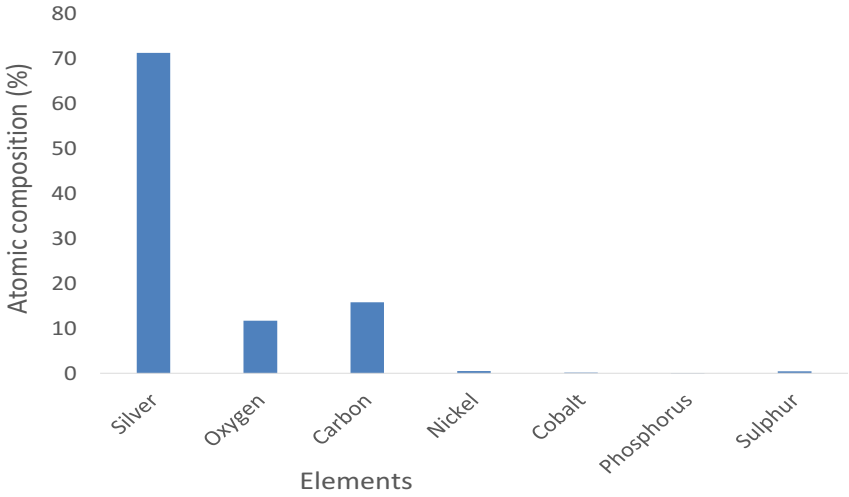

Figure 7:EDX showing the atomic composition of elements present in Ag NPs formed using *M. charantia* stem extract

3.3. *XRD Analysis*

The crystalline nature of the Ag nanoparticles is shown in Figure 8. The intensity of reflection was similar to that of chemical synthesis reported [21]. The Ag NPs were highly crystalline as depicted by X-ray diffractogram. Characteristic reflections which appeared at 2θ values of 38.17^{o}, 44.39^{o},64.57^{o} and 77.49^{o}were indexed to {111}, {200}, {220} and {311} Ag planes of the face-centered cubic structure. The nanocluster reflection displayed peaks with strong intensity, suggesting high purity of the Ag. The XRD diffraction pattern in Figure 8 shows highly crystalline nanoparticles of about 25 nm. The crystallinity is corroborated by the SAED ring pattern (Figure 4a).

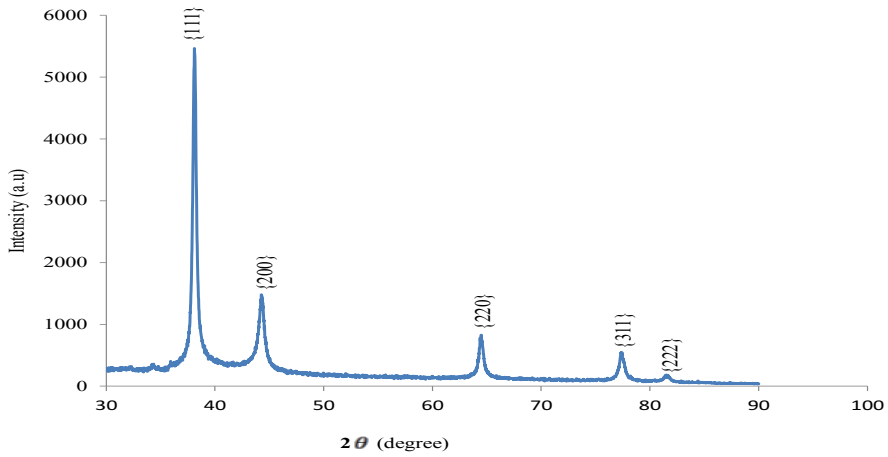

Figure 8: XRD patterns of the Ag NPs prepared using extract of *M. charantia* stem

3.4. *FTIR Analysis*

Evidence of nanocluster capping by the biomolecules is corroborated by the FTIR analysis (Figure 9). The spectrum shows presence of hydroxyl groups (-OH) stretching, (-CH) stretching, C=C stretching and C-N group in the bioactive chemicals that capped the nanoparticles at 3237, 2913, 1620 and 1021 cm^{-1} respectively [22]. The phytochemical screening indicated the existence of saponins and the alkaloids in the stem extract of *M. charantia*, similar to previous work [23]. The presence of C-N proposes coordination through the lone pair electron present in the nitrogen attached to the methyl group, hereby leading to the formation of double bond as Ag^{+} is reduced to Ag^{0}. Capping of the nanoparticles by phytochemicals present in the plant extract provided stability. Proposed mechanisms of the reactionsareillustrated in Schemes 1 and 2.

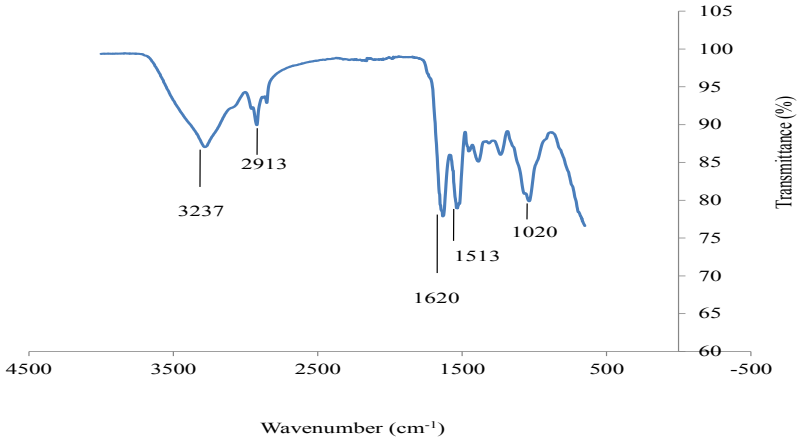

Figure 9: FTIR spectrum of the synthesized Ag NPs using the extract of *M. charantia* stem

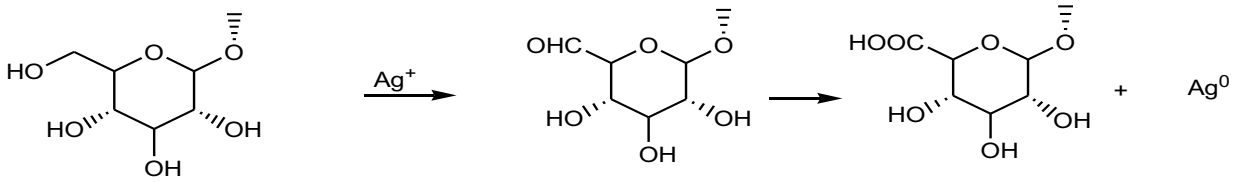

Scheme 1: Bioreduction of silver ionto silver nanoparticles by saponins

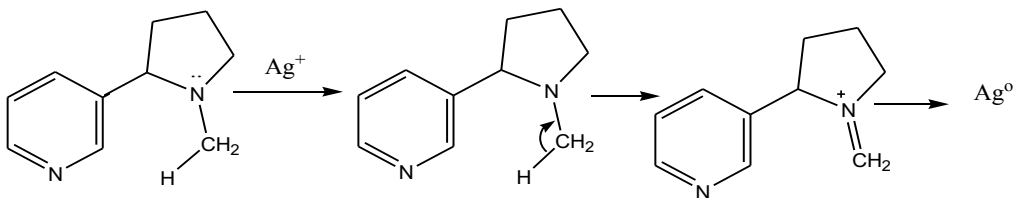

Scheme 2: Bioreduction of silver ionto silver nanoparticles by alkaloids

Conclusions

A rapid, facile and environmental-friendly synthesis of monometallic Ag nanoparticles by green plant-mediated method was successfully achieved via reduction of $AgNO_3$. Consequently, characterization of the prepared nanoparticles was carried out using optical spectroscopy, X-ray diffraction, electron microscopy, selected area electron diffraction, elemental mapping, Fourier transform infra- red. No doubt, interaction of the particles with light showed that they are optically active, as observed in the colour intensity and the UV-Visible result displaying surface plasmon resonance features of monometallic Ag NPs. Evidence of nanoparticle synthesis has been proven based on morphology and size measurement. Quasi-spherical nanoparticles measured 27.81 ± 1.64 nm. Capping of nanoparticles which provided stability was revealed by FTIR result. The hydroxyl groups (-OH) stretching and C-N group in the phytochemicals acted as the reducing/capping agent. Hence; the red shift, strong intensities of absorption and emission are good pointers of the Ag nanoparticles as potential optical materials.

Acknowledgments- The authors wish to thank Mr. OlusolaRotimi ofthe University of Western Cape, Bellvillle campus, Cape-Town, Mr. Shitole Joseph ofiThembaLabssand Mr. OlufemiOlaofe in South Africa for the morphological characterization.

References

1. O. Kvítek, J. Siegel, V. Hnatowicz, V. ŠvorIík, *J. Nanomater.*, 2013 (2013) 15 pages. Article ID 743684.
2. P.K. Jain, S. Eustis, M.A. El-Sayed, *J. Phys. Chem. B.* 110(2006) 18243 doi: 10.1021/jp063879z
3. R. Bukasov, J.S. Shumaker-Parry, *Nano Lett.*7 (2007) 1113.
4. A. Dmitriev, T. Pakizeh, M. Käll, D.S. Sutherland, *Small.* 3 (2007) 294. doi:10.1002/smll.200600409.
5. W. Haiss, N.T.K. Thanh, J. Aveyard, D.G. Fernig, *Anal. Chem.*, 79 (2007) 4215.
6. Y. Sun, Y. Xia, *Science,* 298 (2002) 2176. doi: 10.1126/science.1077229.
7. P. Kumbhakar, S.S. Ray, A.L. Stepanov, *J. Nanomater.,* 2014 (2014) 8 pages. Article ID 181365.
8. N. Ahmad, S. Sharma, V.N. Singh, S.F. Shamsi, A. Fatma, B.R. Mehta, *Biotechnol. Res. Int.,* (2011) 8 pages.
9. D. Mandal, M.E. Bolander, D. Mukhopadhyay, G. Sarkar, P. Mukherjee, *Appl. Micro.Biotech.*, 69 (2006) 485.
10. A. Mourato, M. Gadanho, A.R. Lino, R. Tenreiro, *Bioinorg. Chem. and Appl*. (2011), 8 pages. Article ID 546074. doi:10.1155/2011/
11. M. Apte, D. Sambre, S. Gaikawad, *AMB Express,* 3 (2013) 32.
12. G. Singaravelu, J.S. Arockiamary, V.G. Kumar, K. Govindaraju, *Colloids Surf B: Biointerfaces*, 57 (2007) 97.
13. A.A. Akinsiku, K.O. Ajanaku, J.A. Adekoya, E.O. Dare, *Proceedings of* 2nd Covenant University International Conference on African Development Issues. (2015) 154.
14. R.N. Yadav, M. Agarwala, *J. Phytol.* 3 (2011) 2075.
15. N. Ahmad, S. Sharma, *GSC.*, 2 (2012) 141.doi: 10.4236/gsc.2012.24020.
16. G.B. Sergeev, *Usp. Khim.,*70 (2001) 809.
17. A.M. Smith, H. Duan, M.N. Rhyner, G. Ruan, R. Nie, *Phys. Chem. Chem. Phys.,* 8 (2006) 3895. doi:10.1039/b606572b.
18. J. Yang, R. Wang, L. Yang, *J. Alloy Compd.*, 509 (2011) 3606.
19. R.F. Wang, H. Wang, B.X. Wei, W. Wang, Z.Q. Lei, *Int. J. Hydrogen Energ.*35 (2010) 10081.
20. G. Heimel, M. Daghofer, J. Gierschner, J. Emil, C. Andrew, D. Beljonne, E. Zojer, *J. Chem. Phys.* 122 (2005) 054501. doi: 10.1063/1.1839574.
21. E.O. Dare, O.W. Makinde, K.T. Ogundele, G.A. Osinkolu, Y.A. Fasasi, I. Sonde, J.T. Bamgbose, M. Maaza, J. Sithole, F. Ezema, O. Adewoye, *ISRN Nanomater.*(2012) 8 pages. doi:10.5402/2012/3769.
22. J. Coates, Interpretation of Infrared Spectra, A Practical Approach. John Wiley & Sons Ltd. (2008) pp. 1-23.
23. A.A. Akinsiku, E.O. Dare, K.O. Ajanaku, J.A. Adekoya, S.O. Alayande, A.O. Adeyemi, *J. Bionanosci.* 10 (2016) 171.